UNIVERSIDADE DE SÃO PAULO
INSTITUTO DE GEOCIÊNCIAS

Evolução metamórfica e metassomática do W-skarn do Distrito Mineral de Bodó, Província Mineral Seridó (Província Borborema)

DINARTE LUCAS

Dissertação apresentada ao Programa de Pós-Graduação em Geoquímica e Geotectônica do Instituto de Geociências para obtenção do título de Mestre em Ciências

Área de concentração: Geotectônica

Orientadora: Maria Helena Bezerra Maia de Hollanda

SÃO PAULO
2023

Serviço de Biblioteca e Documentação do IGc/USP
Ficha catalográfica gerada automaticamente com dados fornecidos pelo(a) autor(a)
via programa desenvolvido pela Seção Técnica de Informática do ICMC/USP

Bibliotecários responsáveis pela estrutura de catalogação da publicação:
Sonia Regina Yole Guerra - CRB-8/4208 | Anderson de Santana - CRB-8/6658

Lucas, Dinarte
Evolução metamórfica e metassomática do W-skarn do Distrito Mineral de Bodó, Província Mineral Seridó (Província Borborema) / Dinarte Lucas; orientadora Maria Helena Bezerra Maia de Hollanda. -- São Paulo, 2023.
94 p.

Dissertação (Mestrado - Programa de Pós-Graduação em Geoquímica e Geotectônica) -- Instituto de Geociências, Universidade de São Paulo, 2023.

1. Província Borborema. 2. Província Mineral Seridó. 3. Skarn. 4. Modelagem de equilíbrio de fases. 5. Isótopos estáveis de C-O. I. Hollanda, Maria Helena Bezerra Maia de, orient. II. Título.

UNIVERSIDADE DE SÃO PAULO
INSTITUTO DE GEOCIÊNCIAS

Evolução metamórfica e metassomática do W-skarn do Distrito Mineral de Bodó, Província Mineral Seridó (Província Borborema)

DINARTE LUCAS

Orientador: Profa. Dra. Maria Helena Bezerra Maia de Hollanda

Dissertação de Mestrado

Nº 912

COMISSÃO JULGADORA

Dra. Maria Helena Bezerra Maia de Hollanda

Dra.Lena Virginia Soares Monteiro

Dr. Rafael Gonçalves da Motta

SÃO PAULO
2023

Dedico este trabalho a tio Weimar (*in memoriam*), por desde muito cedo me incentivar e me apoiar a seguir estudando.

AGRADECIMENTOS

Nenhum trabalho acadêmico é feito de forma individual e ao longo desse período tive a oportunidade de compartilhar conhecimento e ser ajudado por diversas pessoas.

À minha família, em especial à minha mãe (Ângela), meu pai (Dinarte) e minhas irmãs (Amanda e Dinah), que mesmo distantes sempre me apoiaram e fizeram de tudo para que eu consiga seguir meu caminho. Seu incentivo sempre foi fundamental para que eu siga na jornada acadêmica mesmo com todas as a dificuldades que vêm com ela. Sou muito grato e amo muito vocês!

À minha orientadora, professora Maria Helena, pela confiança e por ter aberto as portas (inclusive de casa) para mim e dado todo o necessário para que essa pesquisa tivesse sucesso. Muito obrigado por todos os conselhos, conversas e confraternizações. Tudo isso foi essencial para meu crescimento pessoal e profissional. No futuro quero ser um pouquinho do pesquisador que você é! Muito obrigado e seguimos juntos!

Aos amigos que fiz em São Paulo, que tornam os dias mais leves, a saudade de casa mais amena e a vida aqui mais divertida. Sou muito grato por terem me acolhido tão bem, meus dias no IGc não seriam os mesmos sem o cafezinho com bis compartilhado na E21. Muito obrigado Elis Figueiredo, Gabi Serejo (obrigado por todas as caronas!), Nazaré Barbosa (Naza), Luiz Dutra, Lucas Ferreira, Carla Felix, Alexandre Ferraz! Sem esquecer dos amigos da sala B11: Oscar, Caio Tavares e Raulindo (Pepeu).

O mesmo se estende aos amigos e companheiros que compartilham a mesma orientadora (ou quase), também conhecidos como a Máfia de Natal: Ravi Sampaio, Alana Dantas, Thiago Rodrigues, Kauê Seoane e Caio Tavares. Muito obrigado por todos os momentos juntos! Sem vocês as reuniões e “workshops” não seriam tão legais.

Aos amigos que deixei em Natal, mas que sempre estão comigo quando preciso: João Victor e Anna Luiza, obrigado por todos esses anos de amizade pelas conversas e por me aguentarem nesses 10 anos. Mesmo cada um morando hoje em um estado, continuamos sempre juntos. Também não posso esquecer de Dalton, que apesar de não gostar de conversar está sempre por perto! Deixo aqui também um agradecimento mais que especial à Isadora, que me deu (!!!) um notebook para que eu trabalhasse no IGc. Amo vocês!

Aos professores que contribuíram de forma direta ou indireta para esse trabalho. A Renato de Moraes por toda disponibilidade e paciência ao me ajudar com as pseudossecões. A Adauto, por me introduzir ao mundo dos skarns, por todas as correções e pela companhia nos campos. A Laécio Cunha de Souza pela imensa ajuda na petrografia durante o período em que estive em Natal.

Aos funcionários da mina Bodó, que tanto me ajudaram enquanto estive lá. A Maurício, por ter dada acesso a mina e a tudo mais que necessitamos. A Júnior, por todo o apoio e prestatividade enquanto estive na mina. A seu Chagas e família, por ter nos guiado pelas galerias da mina e por todas as ocorrências de skarns da região, pelo acolhimento, cafezinhos, almoço e por toda a disposição em sempre nos ajudar. Sem você esse trabalho com certeza não seria o mesmo.

Aos funcionários do IGc, desde a secretaria até os técnicos de laboratório, todos são fundamentais para que os alunos de consigam dar andamento aos seus trabalhos. Em especial, ao Vasco, Katherine, Claudio, Samuel (Samuca), Paulinho, Marcos Mansueto, Kei Sato, Isaac Sayeg e tantos outros.

RESUMO

O distrito mineral de Bodó compreende uma sequência de mármores metassomatizados e lentes de skarns de W-(Mo) localizados na Faixa Seridó, porção norte da Província Borborema, onde se encontra o depósito de Bodó, um dos depósitos de skarn mais importantes da Província Mineral de Seridó (PMS). Neste estudo, utilizamos uma abordagem multidisciplinar para investigar a evolução metamórfica e metassomática dos skarns e mármores do distrito de Bodó utilizando datações U-Pb e Ar-Ar, isótopos estáveis de carbono e oxigênio e modelagem termodinâmica. O distrito está espacialmente relacionado a granitos e pegmatitos ediacarano-cambrianos, que forneceram idades U-Pb SHRIMP em zircão de 536,6 ± 3,4 Ma para o granito Macambira e idade de $^{40}Ar/^{39}Ar$ em muscovita de 501,63 ± 0,59 Ma para um dique de pegmatito. Em contraste, a idade da mineralização é limitada por uma idade Re-Os em molibdenita (510 ± 2 Ma). Embora não corresponda a nenhuma das idades obtidas para granitos ou pegmatitos no distrito, a idade do skarn é consistente com as idades U-Pb em columbita-tantalita (515-509 Ma) obtidas para outros pegmatitos da PMS, as quais são considerados idades de cristalização, enquanto as idades de Ar-Ar são interpretadas como idades de resfriamento. Assim, os pegmatitos são considerados as fontes ígneas mais prováveis para a formação de skarns. As lentes de mármore da Formação Jucurutu não sofrem mudanças isotópicas significativas durante o metamorfismo regional, enquanto os dados de isótopos estáveis de C-O para calcitas de mármores e skarns do distrito de Bodó indicam uma tendência de empobrecimento em $\delta^{18}O$ consistente com um modelo de interação fluido:rocha. Os dados sugerem uma interação com fluidos magmáticos em uma ampla faixa de valores de XCO_2 e com diferentes taxas de interação fluido:rocha. A modelagem de equilíbrio de fases usando pseudosseções isobáricas T-XCO_2 permitiu estimar as condições de metamorfismo de contato de mármores com diferentes assembleias de minerais silicáticos. As condições de pico metamórfico foram estimadas em 650-600°C, com uma ampla faixa de valores de XCO_2 (entre 0,4 e 0,8), enquanto a fase retrógrada começa em 575-550°C. A cristalização de granada requer um baixo XCO_2 (abaixo de 0,2), indicando um alto influxo de H_2O. Em comparação, a cristalização de escapolita requer um alto teor de XCO_2 (aproximadamente 0,8) que pode ocorrer em condições isotérmicas. Combinadas com observações texturais, essas características sugerem a atuação de um sistema aberto com composições variáveis de fluido.

Palavras-chave: Província Borborema, Província Mineral Seridó, Skarn, Modelagem de equilíbrio de fases, Isótopos estáveis de C-O, Geocronologia

ABSTRACT

The Bodó mineral district comprises a sequence of metasomatized marbles and W-(Mo)-skarn lenses located in the Seridó Belt, northern Borborema Province, in which the Bodó deposit is located, one of the most important W-skarn deposits of the Seridó Mineral Province (SMP). In this study, we employ a multidisciplinary approach to investigate the metamorphic and metasomatic evolution of the Bodó district skarns and related marbles using U-Pb and Ar-Ar dating, carbon and oxygen stable isotopes and thermodynamic modeling. The district is spatially related to Ediacaran-Cambrian granites and pegmatites, which provided U-Pb SHRIMP in zircon age of 536.6 ± 3.4 Ma and $^{40}Ar/^{39}Ar$ in muscovite age of 501.63 ± 0.59 Ma, respectively. In contrast, the age of the mineralization is constrained by a Re-Os age in molybdenite (510 ± 2 Ma). Although these ages are not coeval with any granite or pegmatite ages in the district, the skarn age is consistent with U-Pb ages in columbite-tantalite (515-509 Ma) for other pegmatites in the SMP, which are assumed to be crystallization ages. In contrast, the Ar-Ar ages are interpreted as cooling ages. Thus, the pegmatites are the most likely igneous sources for skarn formation. Jucurutu marble lenses do not undergo significant isotopic changes during regional metamorphism, whereas C-O stable isotope data for calcites of marbles and skarns from Bodó district indicate a heavy $\delta^{18}O$ depletion trend consistent with a fluid:rock interaction model. The data suggest an interaction with magmatic fluids in various XCO_2 values and at different fluid:rock ratios. Phase equilibrium modeling using isobaric T-XCO_2 pseudosections allowed estimate the contact metamorphism conditions of marbles with different silicate mineral assemblages. Peak conditions were estimated at 650–600°C with a wide range of XCO_2 values (between 0.4 and 0.8), whereas the retrograde stage starts at ~500°C. Garnet crystallization requires a low XCO_2 (< 0.2), indicating a high H_2O influx. In comparison, scapolite crystallization requires a high XCO_2 content (approximately 0.8) that may occur at isothermal conditions. Together with the interpretation of textural relantionship, these features suggest an open system setting with varying fluid compositions.

Keywords: Borborema Province, Seridó Mineral Province, Skarn, Phase equilibrium modeling, C-O stable isotopes, Geochronology

SUMÁRIO

1 INTRODUÇÃO

1.1 Apresentação

Depósitos do tipo skarns têm sua relevância atrelada ao fato de serem a principal fonte de metais como o tungstênio (W), além de serem importantes fornecedores de outros metais como Au, Cu, Fe, Mo, Zn, Sn e Pb. No Brasil, a exploração de skarns mineralizados em W está diretamente atrelada à Província Mineral do Seridó (PMS), que engloba grande parte da Faixa Seridó – sequência supracrustal de idade neoproterozoica localizada na porção setentrional da Província Borborema (Van Schmus et al., 2003), nos estados do Rio Grande do Norte e da Paraíba. Essa região encerra uma gama de ocorrências minerais, entre as quais destacam-se pegmatitos mineralizados em Nb-Ta-(Li), ETR e gemas (p.ex., turmalina Paraíba; Beurlen et al., 2008, 2014), esmeralda em rochas ultramáficas (Santiago et al., 2019), ouro orogênico e formações ferríferas bandas (banded iron formation - BIF) (Cavalcante et al., 2016). Por ser um metal estratégico e de grande aplicação, a procura por W foi alavancada durante a Segunda Guerra Mundial, e desde a década de 1940 já foram mapeadas mais de 700 ocorrências de skarns em uma área de aproximadamente 20.000 km² (Santos et al., 2014).

A presente dissertação, vinculada ao Programa de Pós-Graduação em Geotectônica do Instituto de Geociência da Universidade de São Paulo (IGc-USP), envolve o estudo do distrito mineral de Bodó, que apresenta um conjunto de ocorrências de skarns mineralizados em W-(Mo). O distrito está alojado em um sistema de dobramentos sinclinais e anticlinais que afetam as unidades de embasamento regional (gnaisses do Complexo Caicó, de 2,25 a 2,15 Ga; Hollanda et al., 2011) e rochas metassedimentares (micaxistos, mármores e paragnaisses) do Grupo Seridó (Jardim de Sá et al., 1995), que dá nome à faixa de dobramentos Seridó. No distrito, a maior ocorrência é a de Bodó, no extremo leste do distrito, onde a mina está em funcionamento desde a década de 40. Os poucos trabalhos existentes sobre o depósito restringem-se a trabalhos básicos de conclusão de curso, relatórios técnicos e resumos em simpósios ou congressos (Legrand et al., 1994a, 1994b; Costa, 1995; Cavalcante et al., 2016). Apesar da importância econômica reconhecida desse depósito, a evolução metassomática desta mineralização, bem como suas condições de formação e relações espaciais e genéticas com corpos graníticos e

diques pegmatíticos localmente mapeados ainda não estão claras. Assim, os novos dados apresentados nesse trabalho representam uma grande contribuição ao entendimento dos processos associados à gênese dos skarns da PMS.

1.2 Justificativas e Objetivos

Apesar de sua importância local e regional, o distrito de Bodó carece de estudos detalhados que definam suas características petrográficas e químicas, principalmente quando comparado com os outros depósitos melhor estudados da PMS (e.g. Brejuí, Bonfim e Itajubatiba). Muito se especula sobre a relação genético-temporal entre os skarns e a granitogênese ediacarana-cambriana. As contribuições mais recentes sobre essa questão referem-se a idades precisas que vêm sendo obtidas tanto para os corpos ígneos regionais como para os skarns. No distrito de Bodó, uma idade Re-Os em molibdenita de 510 ± 2 Ma (Hollanda et al., 2017) não encontra correspondência com corpos graníticos datados na região (Archanjo et al., 2013; Hollanda et al., 2015, 2017; Souza et al., 2016), evidenciando a necessidade de se rever o modelo genético-temporal até então aceito para a região. Muito pouco é sabido sobre as condições de pressão e temperatura vigentes durante a formação dos skarns a partir de mármores encaixantes, bem como as características dos fluidos metassomáticos associado à sua formação.

Os objetivos deste trabalho são:

- Compreender a relação temporal entre a mineralização e corpos ígneos por meio da obtenção de idades de granitoides (U-Pb SHRIMP em zircão) e pegmatitos (Ar-Ar em muscovita) existentes no entorno do distrito/depósito de Bodó;
- Caracterizar a evolução temporal relativa do depósito e a composição química das principais fases minerais presentes nos skarns e mármores do distrito de Bodó;
- Identificar a origem dos fluidos hidrotermais na interação com os protólitos carbonáticos dos skarns, através das composições de isótopos estáveis de carbono e oxigênio;
- Caracterizar as condições de T-XCO_2 envolvidas na formação dos mármores e skarns, através de modelagem termodinâmica.

1.3 Estrutura da Dissertação

Seguem-se a este capítulo introdutório, um capítulo de revisão bibliográfica sobre skarns e sobre a aplicação de isótopos de carbono e oxigênio como traçadores de fluidos responsáveis pela formação dessas rochas (Capítulo 2), o texto principal da dissertação (Capítulo 3). Esse último contempla a apresentação dos resultados e interpretações descritos na forma de manuscrito (em elaboração), com foco em descrever as condições de metamorfismo/metassomatismo associadas ao distrito de Bodó, os dados isotópicos de carbono e oxigênio utilizados para modelagem da interação entre o fluido magmático e as rochas carbonáticas encaixantes e, por fim, os dados geocronológicos que visam correlacionar a mineralização à uma fonte ígnea (granitos ou pegmatitos). Ao fim, são apresentadas de forma única todas as referências bibliográficas utilizadas ao longo da dissertação.

2 REVISÃO BIBLIOGRÁFICA

2.1 Skarns: Definition, Genesis and Classification

Skarn is a term of Swedish origin used to name very hard rocks dominated by calc-silicate minerals. Modern literature also uses this term to define rocks composed of calc-silicate minerals, such as garnet, pyroxene and wollastonite, formed due to metasomatic reactions that replace a Ca-rich sedimentary (or metasedimentary) protolith, but it's not limited to them (Zharikov, 1970a; Meinert, 1992; Meinert et al., 2005; Robb, 2005). Some authors (e.g., Meinert et al., 2005) descriptively use this term based only in the mineralogy of the rock, without a genetic sense.

Skarn's common genesis, however, is related to magmatic (or metamorphic, to a lesser extent) hydrothermal fluids derived from igneous intrusions (Zharikov, 1970a; Chang et al., 2019). When in contact with reactive wall rocks, the fluids may form calc-silicate minerals and economically important metals (Au, Cu, W, Mo, Fe, Sn and Zn) that are also used to name the different deposit types (e.g., W-Mo skarn, Au skarn etc.) (Meinert et al., 2005).

This topic aims to review the main characteristics of skarns, including definitions, classification, and an overview of their mineralogy and chemistry, in addition to metasomatic and zonation processes related to skarn formation. Furthermore, we will present a broad view of the main skarn types combined with some examples of deposits worldwide.

2.1.1 Definitions and terminology

Skarn is commonly classified in exoskarn and endoskarn, the first is formed after sedimentary protolith and the latter formed within the igneous intrusion (Einaudi and Burt, 1982; Meinert et al., 2005). The main pattern observed in endoskarns is the influx of Ca-rich material into the protolith. Under reduced conditions, the paragenesis towards limestone is formed by biotite, amphibole, pyroxene and ± garnet; pyroxene-plagioclase is the diagnostic assemblage in this case. Under more oxidized conditions, epidote-quartz and abundant garnet are the main features (Einaudi and Burt, 1982).

However, distinguishing between endo- and exoskarn can be a challenge when skarns are massive or when primary textures are completely overprinted by late

hydrothermal alteration. According to Mrozek et al. (2020), a strategy to overcome this problem is using whole-rock geochemistry and comparing the composition of skarns and their respective wall rocks and igneous intrusive rocks. Aluminum, HREE and HFSE are typically immobile during skar formation and are mainly derived from precursor rocks. Thus, comparing the immobile element content allows the characterization of the sharn's precursor and distinguish between endoskarn and exoskarn.

Concerning its chemical composition, exoskarns can be calcic or magnesian depending on the original wall rock (limestone or dolostone, respectively) (Einaudi, 1982; Einaudi and Burt, 1982; Ray and Webster, 1991). Limestone with low MgO typically forms Ca-skarns with garnet, wollastonite, vesuvianite, clinopyroxene and epidote. With increasing MgO content in limestone, skarns are likelier to have Mg-bearing minerals as diopside and phlogopite. Proper Mg-skarns, though, will present Mg-rich minerals such as forsterite, spinel, humite and rare phlogopite and diopside (Zharikov, 1970a, 1970b; Chang et al., 2019). Under moderate *P-T* conditions and increasing CaO activity at retrograde stages Mg-skarns may be replaced by Ca-skarns (Zharikov, 1970b).

The morphology of skarns depends on different factors such as the size of the hydrothermal system, the permeability of host rocks and the existence of structural controls (e.g., faults and fractures) (Ray and Webster, 1991). Ray and Webster (1991) defined three morphological types based on the occurrences in British Columbia (Canada) and the Nambija deposit (Ecuador).

The first one, pervasive and massive exoskarns envelopes (Figure 1a) are formed near the causative intrusion. The alteration zones overprint subjacent lithologies and are mainly controlled by the morphology of the intrusive rock, in which case structures have only minor importance. The second type refers to vein-related skarns, usually composed of veins of sulfides or quartz enveloped by pervasive skarn alteration (Figure 1b). Pre-existing structures intrinsically control this morphology as the source of the fluids – the causative intrusion – may not be close. The third type is the stratiform skarns, which is marked by the lithological concordance (Figure 1c). Due to its nature, they occur as thin bodies within extensive zones following a preferred stratigraphic horizon.

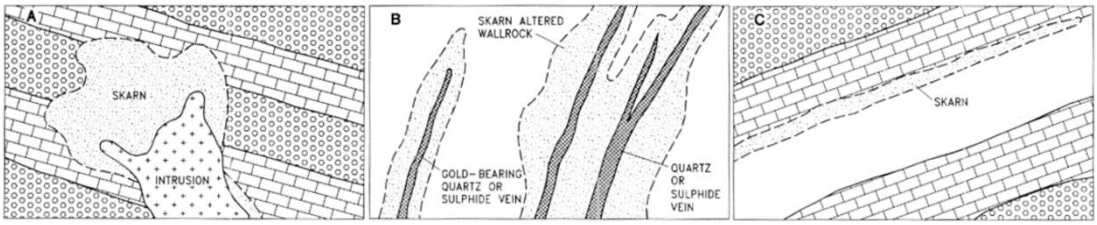

Figure 1 – Main morphological types of skarns. A) Pervasive and massive skarn. B) Vein-related skarn. C) Stratiform skarn. Source: Ray and Webster (1991).

2.1.2 Metasomatism and metasomatic zonation

2.1.2.1 Metasomatic Processes

Metasomatism is a metamorphic process in which the composition of a rock is altered by the interaction with aqueous fluids that drives elemental leaching or enrichment . In this process, the rock remains in a solid state (Lindgren, 1925; Zharikov et al., 2007). The main principles of metasomatism and metasomatic processes were derived from works by Korzhinskii and were summarized in the Theory of Metasomatic Zoning (Korzhinskii, 1968). The author formulated a variation of the phase rule considering mobile and immobile components (Thompson, 1959; Korzhinskii, 1965). The mobile components are the ones introduced or removed in the system and their chemical potential is only controlled by the fluid. However, the immobile (or inert) elements are mainly from the rocks undergoing metasomatism. Following these principles, the phase rule is calculated using only the immobile components. Therefore, the metasomatic assemblages will have fewer phases than those generated by isochemical metamorphism. Korzhinskii defined two main processes of mass transfer during metasomatism: diffusion and infiltration. Although both are different mechanisms, they can be considered as end-members of the same spectrum and their combination is more common in most natural processes.

The diffusion metasomatic process is related to the transport of components through a stationary (or stagnant) fluid. The driven force of diffusion is the chemical potential gradients (Zharikov et al., 2007). Thus, reactions may occur between rock components and diffusing components, but direct precipitation cannot occur as the elements migrate to areas of low activity. Following these principles, the migration of components will appear from the zone with higher chemical potential to the lower one. As the concentration of the pore solution changes at the limit of every alteration zone,

the composition of formed minerals may change gradually within it. Transport by diffusion is limited to short distances, usually on a decimeter or centimeter scale and barely on a meter scale. The diffusional process tends to form reaction rims along fissures, veins and contact surfaces, showing gradual compositional variations. During diffusion, chemical components can migrate in opposite directions in a process called bimetasomatism that occurs in a contact between two rocks in chemical disequilibrium.

In infiltration metasomatism, the transfer of material in solution occurs during percolation or infiltration of the fluid through the rocks. The movement of fluid during the infiltration process is driven by pressure and concentration gradients between external fluid and the rock-pore solution (Zharikov et al., 2007). As opposed to diffusion, the chemical potential is constant over the entire zone, and so the composition of minerals that form solid solutions is stable. Furthermore, the metasomatic zones are more spatially expansive extending for several meters. In infiltration, all compounds move following the same direction and minerals can be directly precipitated, unlike diffusion metasomatism.

2.1.2.2 Skarn Zonation

Most skarns present a typical temporal and spatial (from proximal to distal) zonation regarding the fluid source (Korzhinskii, 1968; Meinert, 1997; Chang and Meinert, 2008). The development extension of the metasomatic front is directly related to the volume of fluid channeled in the system (Meinert et al., 2005). The reactions driven force is mainly the chemical potential or activity gradient in response to changes in temperature and pressure (Kwak, 1987). Thus, the magnitude of chemical potential gradients depends on these variables' rate of change. Usually, a sharp front separates different mineral assemblages that are not in equilibrium and each zone represents the stability field of each assemblage (Korzhinskii, 1968; Kwak, 1987).

A more significant variation of skarn zones occurs due to differences in mobility for each component. For example, silica is more soluble, travelling faster and further than less soluble elements. In Figure 2, each front represents different mobility for the main components of the fluid. Wollastonite corresponds to Si metasomatism; pyx > grt indicates Fe ± Mg metasomatism, while grt > pyx front indicates Al transport (Meinert et al., 2005). When the fluid flow is slow, zoned skarns are formed, whereas a rapid

fluid flow most likely tends to form unzoned skarns, which later can be overprinted by slower travelling reactions. Usually, most skarns are between these two end-members (Kwak, 1987).

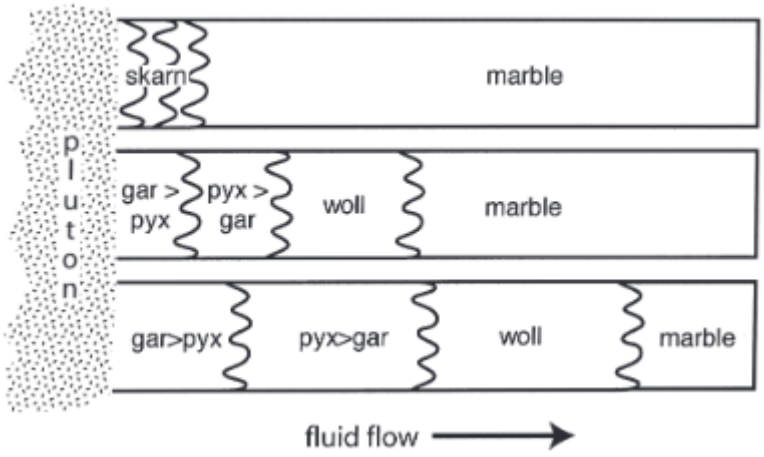

Figure 2 – Propagation of multiple reaction fronts due to fluid flow from the igneous rock. Mineral predominance indicates different metasomatic patterns and different mobility of fluid components (e.g., SiO_2, Al, Fe, Mg). gar = garnet, pyx = pyroxene, woll = wollastonite. From Meinert et al., (2005).

It's important to note that during the formation of zoned skarns, some parts could have constant pressure and temperature but variable activity (Kwak, 1987). Therefore, simple *P-T* or *T-XCO₂* cannot always be sufficient to represent the conditions for the genesis of zoned skarns. For these cases, relevant diagrams are the ones in which the activities of important elements are variable while pressure and temperature are fixed. In Figure 3, for instance, mineral stability for different values of SiO_2 activity is shown in the $CaO\text{-}SiO_2\text{-}MgO\text{-}Al_2O_3\text{-}H_2O\text{-}CO_2$ system at 425°C, 0.5 kbar and $XCO_2 = 0.007$. In all diagrams in Figure 3, the point "X" has the same values for both axes, but the silica activity varies. Just this variation can produce three different zones: clinozoisite + diopside (Figure 3a), garnet + clinozoisite (Figure 3b) and garnet only (Figure 3c).

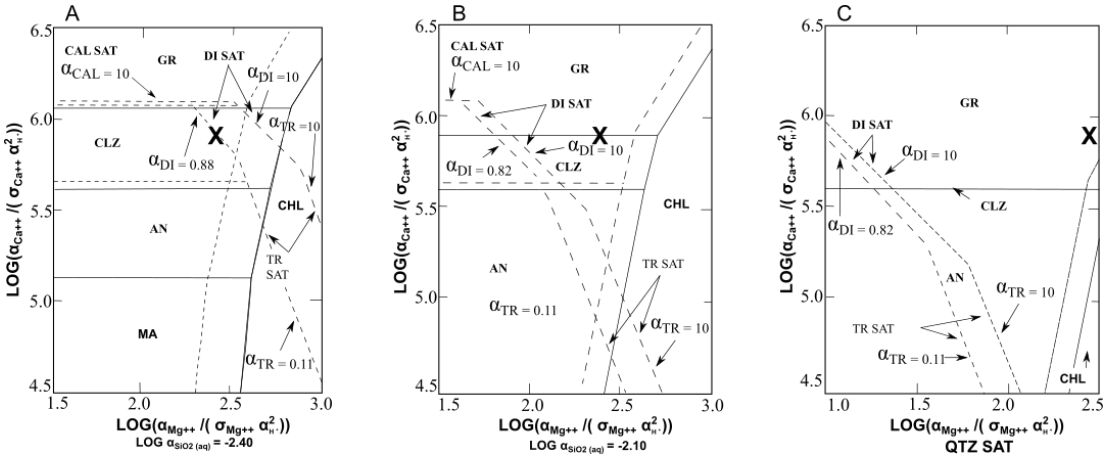

Figure 3 – Log activity diagrams for the system $CaO\text{-}SiO_2\text{-}MgO\text{-}Al_2O_3\text{-}H_2O\text{-}CO_2$ at 425°C, P = 0.5 kbar and $XCO_2 = 0.007$. Every diagram shows major changes in mineral stability due to different silica activity. Silica activity = -2.40, -2.10 and at quartz saturation in A, B and C, respectively. Point "X" is at a constant position in all three diagrams. WOL = wollastonite, TR = tremolite, FO = forsterite, ANT = antigorite, QTZ = quartz, MA = margarite, CO = corundum, WA = wairakite, PYR = pyrophyllite, PREH = prehnite, GR = garnet, AND = andalusite, CLZ = clinozoisite and CHL = chlorite. Form Kwak (1987) after Frisch and Helgeson (1984).

2.1.3 Stages of skarn formation

Skarns are formed by a sequence of different processes (Ray and Webster, 1991; Meinert, 1992; Meinert et al., 2005) (Figure 4 and Figure 5) which may be seen almost entirely in some deposits (e.g., Phu Lon Cu-Au deposit; Kamvong et al., 2006). The first one – isochemical crystallization – occurs in a prograde stage due to contact metamorphism caused by the intrusion of magma, which can form hornfels (Figure 4A). In this stage, there is no significant mass transfer (no change in bulk composition) with recrystallization and changes in mineral stability as the main process. The new mineral assemblage is conditioned by the composition of the wall rocks (Meinert et al., 2005) and no mineralization is formed.

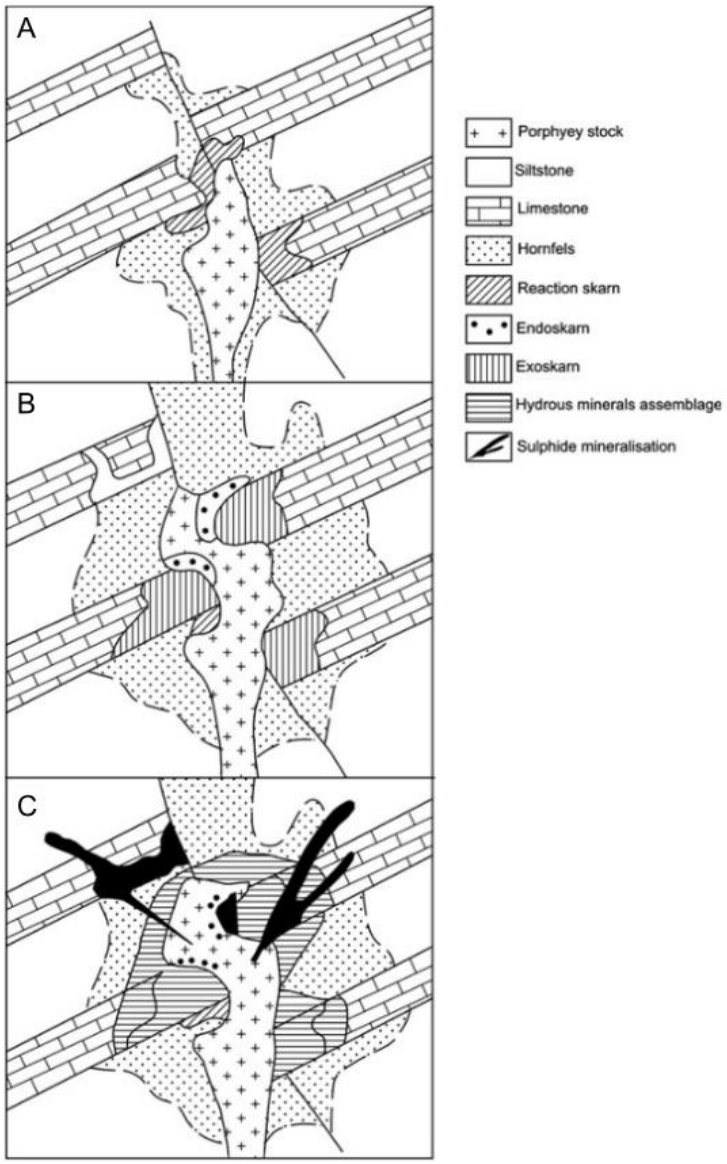

Figure 4 – Stages of skarn formation. A) Isochemical stage with the development of hornfels in non-carbonate lithologies and beginning of reaction skarn formation in carbonates. B) Main metasomatic stage with development of exo- and endoskarns. C) Retrograde stage in which skarns from the prograde stage could be overprinted. Hydrous minerals and sulfides dominate this stage. From Pirajno (2013).

Metasomatic reactions between different lithologies – or at the contact thereof – such as limestone and shale result in the formation of metasomatic rocks by a process known as bimetasomatism (Figure 4B) (Korzhinskii, 1968; Zarayskiy et al., 1987; Zharikov and Rusinov, 2015). This stage involves the transfer of Ca from the carbonate-rich lithology towards the poor one. On the other hand, elements such Al, K, Na, Fe, Mg and Si follow the opposite path (Meinert et al., 2005). Studies in major W-Sn skarn deposits from China (Huangshaping, Shizhuyuan and Xianghualing skarns) indicate that Si, Al and trace elements in skarns are controlled by the source

granite while Ca, Mg, Mn, Ti, Sr and REE are mostly derived from the host rocks (Jiang et al., 2018).

As part of this prograde stage, the infiltration of magmatic-hydrothermal fluids (H_2O and CO_2 saturated) derived from the intruding magma leads to the formation of infiltration skarns (as stated by Einaudi and Burt, 1982) or pure metasomatic skarns (Figure 4B; Figure 5). These resulting rocks do not necessarily reflect the protolith composition. The prograde assemblage is formed at high-temperature from 400°C to >700°C (Meinert et al., 2005; Buriánek et al., 2017; Chang et al., 2019). Some important economic minerals, such as scheelite and magnetite, could be formed in this stage (Robb, 2005).

The last stage occurs after the system's cooling when meteoric water infiltration causes retrograde metamorphic reactions (Figure 4C; Figure 5) (Einaudi and Burt, 1982). This stage is associated with the precipitation of sulfides and other metals. The retrograde alteration is usually more intense and pervasive at shallower depths (Meinert, 1992; Meinert et al., 2005) and can obliterate the previous mineralogy. Otherwise, the metal precipitation connected to processes like reduction of the fluids' solubility due to a decrease in temperature, fluid mixing and neutralization of the ore fluid when in contact with carbonate lithologies (Robb, 2005).

Skarnoid is an intermediate calc-silicate rock between hornfels and a pure reaction skarn. This rock is not entirely overprinted by hydrothermal alteration and thus reflects the mineralogy of the host rock (Meinert, 1992; Meinert et al., 2005). Skarnoids are usually Fe-poor and fine-grained.

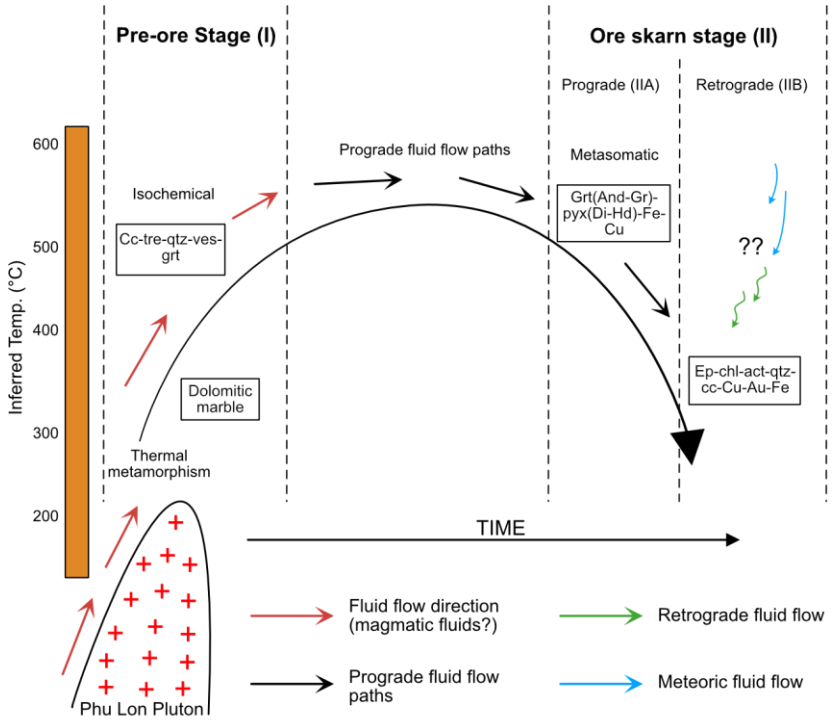

Figure 5 – Schematic evolution, paragenesis and interpreted fluid paths throughout time in Phu Lon Cu-Au deposit, Thailand. Act = actinolite, and = andradite, cc = calcite, chl = chlorite, di = diopside, ep = epidote, gr = grossular, grt = garnet, hd = hedenbergite, pyx = pyroxene, qtz = quartz, tre = tremolite, ves = vesuvianite. From Kamvong et al., (2006).

2.1.4 Skarn types and main deposits

Skarns deposits are divided according to the metal association. The most known and well-studied are Au, Cu, W, Mo, Fe, Sn and Zn skarns (Meinert et al., 2005). Nevertheless, more than one metal may occur associated in the same deposit (e.g., W-Mo, W-Sn, Cu-Au, Zn-Pb and so on). Ray and Webster (1991), Meinert (1992), and Meinert et al. (2005) summarized the general features of important skarn deposits worldwide. Some authors (e.g., Ray and Webster, 1991) suggest a correlation between the main metal and magma differentiation processes, which are related to magma source and tectonic settings.

For simplification purposes, a broad view of main characteristics and some examples of W skarn deposits type is presented.

2.1.4.1 Tungsten Skarns

Tungsten is a strategic metal due to its characteristics (e.g., hardness, corrosion resistance, density and resistance to high temperature) that make it of great value for industrial use. Generally, tungsten of hydrothermal origin is related to highly differentiated peraluminous granites derived from the melting of sedimentary rocks, indicating crustal origin (Hulsbosch et al., 2016; Romer and Kroner, 2016). The mechanism of tungsten precipitation can be associated with the depressurization of magmatic fluids (Korges et al., 2018), fluid cooling andmixing (Ni et al., 2015; Legros et al., 2019; Pan et al., 2019) or fluid-rock interactions (Lecumberri-Sanchez et al., 2017). The latter is particularly consistent as the main controlling factor for the precipitation of W in skarns (Legros et al., 2020).

W skarns are generally associated with calc-alkaline plutons with subordinate aplites and pegmatites surrounded by high-temperature metamorphic aureoles (Ray and Webster, 1991; Meinert et al., 2005). The host rocks consist of interbedded carbonates, pelites and occasionally volcanic rocks, similar to those observed in continental margin fore-arc sedimentation (Kwak, 1987). Due to rapid changes in lateral and vertical facies, thick carbonate units and skarn bodies are uncommon (Kwak, 1987). The principal ore mineral is scheelite with subordinate molybdenite, chalcopyrite, cassiterite and sphalerite.

The Cantung deposit (NW Territories, Canada) is an excellent example of world-class W skarn mineralization. Along with Mactung, Lend and other W occurrences, Cantung is part of a large metallogenetic belt that is responsible for the majority of tungsten deposits in North America (Elongo et al., 2020). Two plutons with sub-alkaline biotite monzogranite composition are associated with the mineralization in Cantung skarn: the Mine and the Circular stocks. The first is the main responsible for the mineralization while the latter is more distal. These rocks intrude a sequence of folded quartzites, dolomites, argillites and limestones (Elongo et al., 2020; Legros et al., 2020). The mineralization is formed by structurally controlled skarn lenses and pods with disseminated scheelite replacing Ca-limestones (Legros et al., 2020).

The deposit was formed by reduced fluids with the representative mineral assemblage of grossular and hedenbergite. A reduced environment favors tungsten

extraction from magma to fluid, which could explain the high-grade W mineralization (Candela, 1992). The prograde stage is represented by garnet-pyroxene and pyroxene skarns, while the retrograde stage consists of amphibole and biotite-rich facies (Elongo et al., 2020). Scheelite, however, is distributed among all stages.

Based on fluid inclusion studies, Legros et al. (2020) indicate that the fluids near the intrusion are CO_2-rich and have low Cs and Rb, suggesting they are derived from a less evolved magmatic source. Fluids that interacted with limestones are CH_4-rich, an indicator of a more differentiated source. Scheelite precipitation is related to the interaction between surrounding limestones and magmatic fluid evolved from granite intrusions. This interaction triggered the H neutralization of the magmatic fluid and incorporation of Ca (Legros et al., 2020).

Another world-class example is the Zhuxi W-Cu skarn deposit (Jiangxi, South China), where mineralization is located near biotite monzogranite, fine-grained granite, and granite porphyry. Sr, Nd and Hf isotopes and trace elements modelling indicate that the granites are derived from the dehydration melting process of fertile Neoproterozoic metasedimentary rocks (Song et al., 2018). The prograde skarn mineralogy is formed by garnet, pyroxene, wollastonite and uncommom vesuvianite. The retrograde stage consists of tremolite, vesuvianite, apatite, muscovite, phlogopite, chlorite, scheelite, and rare actinolite, serpentine, fluorite, and epidote. The last hydrothermal event includes scheelite, chalcopyrite, pyrrhotite, sphalerite, fluorite, and galena (Song et al., 2018; Zhang et al., 2021).

2.2 Carbon and Oxygen Isotopic Signature as a Proxy for Tracing the Nature of Skarn-Forming Fluids

Stable isotope methodology has a wide range of applications, such as paleoclimate studies, hydrology, oceanography, planetary science and petrology. Most common elements (i.e., C, H, O, N and S) have more than one stable isotope and all of them can be used in a variety of studies. Isotopes of the same element are similar regarding chemical and physical properties but can be fractionated due to small mass differences during chemical reactions of physical processes (Pat Shanks, 2014). These elements are not the main components of hydrothermal fluids, which makes

them a great tool for understanding fluids and fluid-rock interactions (Rollinson and Pease, 2021).

In contact and regional metamorphic settings, isotope geochemistry can be used to estimate temperature, determine the nature and significance of fluid-rock interactions and fluids' sources, and infer the protolith of metamorphized rocks (i.e., igneous or sedimentary) (Rumble, 1982). This application extends to ore systems related to this type of metamorphism, such as skarn systems, which have its genesis usually related to intrusive igneous rocks close to carbonate-rich lithologies in conjunction with metasomatic processes.

Carbon and oxygen isotopes play an important role in skarn systems, offering insights into their genesis as the contribution of (metasomatic process, purely contact or regional metamorphism), geological processes and evolution. These isotopes are sensitive to volatilization processes and fluid-rock interactions during metamorphism (Taylor, 1974, 1977; Valley, 1986). Thus, this methodology is commonly used to assist the interpretation of ore systems worldwide. This work aims to introduce the main principles for understanding carbon and oxygen systematics and its application to fluid-rock interactions in skarns.

2.2.1 Stable Isotope Systematics

Stable isotope values are normally given as δ (delta), a ratio where the less common isotope is the numerator while the more common one is the denominator. The results, which are always relative to a standard, are given in parts per thousand (or per mill, ‰) and are calculated according to the equation below

$$\delta = \frac{R_{(sample)} - R_{(standard)}}{R_{(standard)}}$$

where R is the abundance ratio between the heavy and light isotopes (e.g., $^{13}C/^{12}C$ or $^{18}O/^{16}O$). A positive value indicates that the sample is enriched in relation to a standard, so it is isotopically heavy. Likewise, a negative value means that the sample is relatively depleted and is isotopically light.

2.2.1.1 Isotope fractionation

Isotope fractionation is the partitioning of an isotope between phases or components with different isotope ratios (Pat Shanks, 2014). The isotopic fractionation factor is given by the α (alpha) value, which is the ratio of isotopes in two substances (A and B), as represented by the following equation:

$$\alpha_{A-B} = \frac{R_A}{R_B}$$

where R is the isotope ratio in substances A and B (e.g., $^{18}O/^{16}O$ in CO_2 for A and $^{18}O/^{16}O$ in calcite for B). Values for α are usually very close to 1 and only vary in the third decimal place (i.e., 1.00X). α can be related to δ following expression:

$$\Delta_{A-B} = \delta_A - \delta_B \cong 1000 \ln \alpha_{A-B}$$

The above equation is a good approximation for when δ values are less than 10. For larger values, the expression should be:

$$\alpha_{A-B} = \frac{1000 + \delta_A}{1000 + \delta_B}$$

There is also a relation between temperature and fractionation factor. In general, the fractionation factor decreases when temperature increases, approaching a value of 1.0. This means that at high temperature isotope fractionation can cease (Faure et al., 2005). The relationship between α and temperature is given by

$$1000 \ln \alpha_{A-B} = \frac{A \times 10^6}{T^2} + B$$

where A and B are experimentally determined constants and T is temperature in Kelvin.

The isotope fractionation factor can be determined through several methods (Pat Shanks, 2014; Rollinson and Pease, 2021). That includes empirical evidence based on natural samples where the formation temperature is well known, experimental isotopic exchange studies, and theoretical calculations based on models of atomic structure and bond strength. The fractionation factor for different minerals was already obtained by several authors over the years and compilations can be found in Bottinga (1969), Zheng (1999), Chacko et al. (2001) and Sharp (2017), among others.

2.2.2 C and O stable isotopes as geochemical tracers in fluid-rock interactions

Stable isotopes have been applied to uncover metamorphic and hydrothermal systems and understand fluid flow and sources (Valley, 1986; Bowman et al., 1994; Baumgartner and Valley, 2001). In these scenarios, processes involving mass transport (including diffusion, fluid infiltration and volatilization), fluid-rock interaction, metasomatism and fluid-driven process are important. Due to their nature, these fluids are also relevant in studies regarding hydrothermal/metasomatic systems and, thus, mineralizing processes that can be associated with them (e.g., skarns). Furthermore, a combined study of carbon and oxygen isotopes in carbonates is a powerful tool to study processes related to the origin and evolution of C-O-bearing fluids.

Relative to fluid migration and interaction during metamorphism, processes can be controlled by the degree to which fluid flow is concentrated into zones of high permeability (Valley, 1986). Two end-members are used to characterize these fluid patterns, as noted by Valley (1986): pervasive and channelized fluids. The first defines fluids that move independently of any structural or lithologic control, permeating all rocks almost equally. This flow type usually occurs along grain boundaries or fine-scale fracture networks and is responsible for homogenizing chemical components, including stable isotopes, in an open system way. On the other hand, channelized fluid occurs along vein systems, shear zones, rock contacts or permeable lithologies. The channelized flow leads to heterogeneous alteration, allowing some rocks to remain unaltered while others are infiltrated and modified (even isotopically). In this situation, close and open system behavior occurs close (Valley, 1986; Baumgartner and Valley, 2001).

According to Valley (1986), in metamorphic systems, the stable isotopic composition is controlled by four factors: the composition of the protolith, the effects of devolatilization, the exchange with infiltrating fluids and the exchange temperature . All these factors were well studied in contact metamorphism environments as the geologic control in these systems is facilitated due to significant differences in the initial isotopic composition of fluids. In these systems, for example, there is usually a significant difference in $\delta^{18}O$ between intrusive rocks and surrounding carbonates,

which makes it easier to understand fluid flow systematics (Baumgartner and Valley, 2001).

2.2.2.1 Metamorphic Volatilization

During prograde metamorphism of sediments, igneous or low-grade metamorphic rocks, volatile components are released by the reaction of low-temperature minerals (Valley, 1986; Baumgartner and Valley, 2001). Dehydration is the most common process, but in carbonate-rich lithologies, decarbonation plays an important role (Valley, 1986). Desulfidation can also be locally significant. For this reason, stable isotopes of C, O, S and H show the most prominent effects of stable isotopes in metamorphic environments.

Volatilization reactions usually cause positive volume changes in the system. As the resulting fluid and solids volume is greater than the initial solids and pore fluids, the differential pressure crested is sufficient for fluid expulsion (Valley, 1986; Baumgartner and Valley, 2001). This migration may occur laterally, downward or upward. According to Valley (1986), most evolved fluids are expelled from their rock of origin and fluid inclusions are the only remnants of these fluids in most scenarios (Baumgartner and Valley, 2001).

The volatilization process and the releasing of fluids out of the system significantly affect the stable isotope composition of residual rocks. Consequently, stable isotope ratios can provide the amount of volatilization that has occurred (Valley, 1986). This phenomenon can be described as a two-end-member process (Valley, 1986): the first, batch volatilization, occurs when all the fluid is evolved before any escape. The second one, Rayleigh volatilization, occurs when each volatile molecule is immediately isolated from the rock of origin. These processes are related to closed and open systems, respectively and most natural cases are between these extremes.

2.2.2.1.1 Batch volatilization

During volatilization in a closed system, the products of phase separation will stay in the reservoir until they are extracted after the process is completed (Hurai et al., 2015). If all the evolved fluid equilibrates with the rock, the resulting isotopic ratio

will be either higher or lower based on whether the fluid partitions preferably the light or the heavy isotopes, respectively (Valley, 1986).

This process is known as batch volatilization (Nabelek et al., 1984), closed system volatilization (Brown et al., 1985) or single-stage volatilization (Bowman et al., 1985). The depletion of the heavy isotope is more common and the following equation can represent the magnitude of this effect:

$$\delta f = \delta i - (1 - F)1000 \ln \alpha$$

Where F is the mole fraction of the element that remains in the rock after volatilization, ranging from 1 (unreacted) to 0 (the element is completely lost to vapor and fluid phase); α is the fluid-rock fractionation factor; δi is the initial and δf is the final isotopic ratio of the rock. Graphically, batch volatilization can be represented by straight lines, as seen in Figure 6.

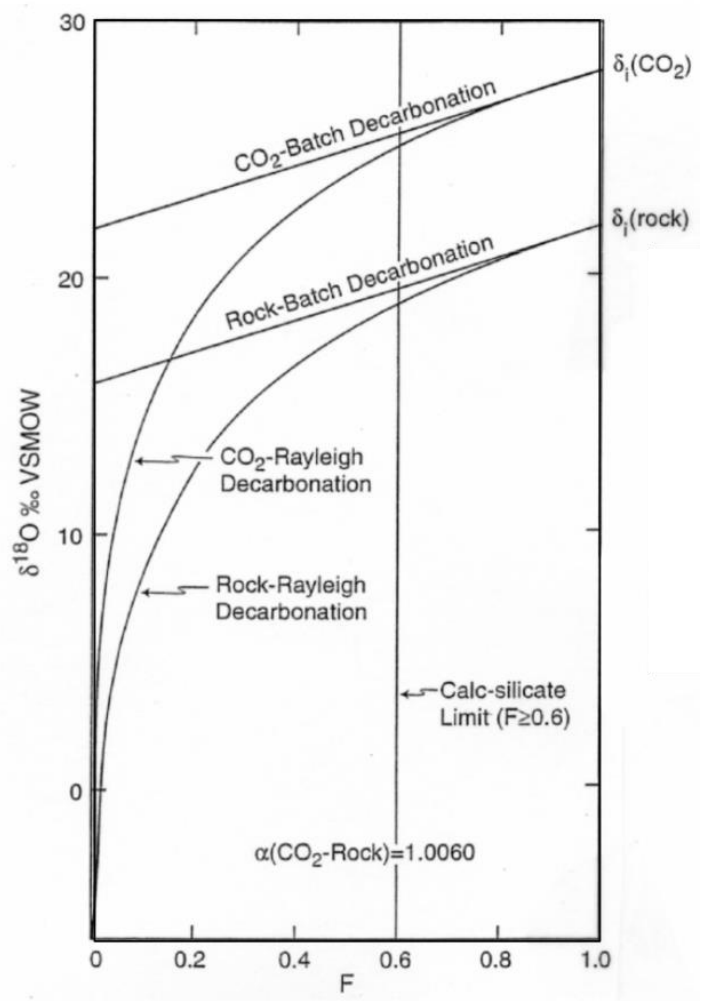

Figure 6 – Changes of $\delta^{18}O$ of rock (δr) and evolving CO_2 fluid (δf). α = 1.0060. Straight lines represent batch volatilization, while Rayleigh volatilization is represented by curves. For high values of F (above

0.6), both volatilization processes have almost the same effect. For oxygen, the maximum degree of reaction for decarbonation reactions is given by the calc-silicate limit. From Baumgartner and Valley (2001).

2.2.2.1.2 Rayleigh volatilization

The Rayleigh volatilization (or distillation) describes the isotopic fractionation process in an open system, where fluids leave the system as they are formed. The continuous removal of small amounts of material in equilibrium with the rock leads to gradual changes in the isotopic composition of the rock and the bulk composition of the residual rock-fluid system (Valley, 1986; Sharp, 2017). The Rayleigh volatilization is a good approximation for the isotopic effects of dehydration and decarbonation (Rumble, 1982; Valley, 1986).

An open system means that fluids and melt can enter and leave the rock. There's no limit to how much fluid can pass through a rock, but the quantity of internally generated fluid that can be lost from the rock is limited (Sharp, 2017). In the lack of fluid or melt entering the rock, the bulk chemistry of the rock limits the amount of fluid that can be released from the system and how much the isotopic composition of the rock can change (Sharp, 2017).

The following equation represent the isotopic change due to Rayleigh volatilization:

$$\delta f - \delta i = 1000(F^{(\alpha-1)} - 1)$$

where δi and δf are the rock's initial and final isotopic ratio, respectively. α is the fluid-rock fractionation factor and F is the mole fraction of the element that remains in the rock after volatilization, ranging from 1 (unreacted) to 0 (the element is completely lost to vapor/fluid phase) in a similar way to what happens in batch volatilization.

In Figure 6, both volatilization end-members represent ^{18}O depletion of siliceous dolomite ($\delta i_{(rock)} = 22$, $\alpha_{(fluid\text{-}rock)} = 1.0060$). It's important to note that for F equal to or higher than 0.6 (calc-silicate limit), the oxygen depletion is similar in both volatilization processes. At even lower F values, however, depletion caused by Rayleigh fractionation becomes more significant.

For simple decarbonation reactions such as the formation of wollastonite and release of CO_2 from calcite and quartz:

$$CaCO_3 + SiO_2 \rightarrow CaSiO_3 + CO_2$$

a maximum of 40% of the oxygen in the reactants can be released to the fluid phase. This implies that F cannot decrease below 0.6, the calc-silicate limit (Valley, 1986). This limit is attached to the fact that silicate minerals are the dominant oxygen reservoir in the residual metamorphic rock even after volatilization. Thus, values of oxygen below the calc-silicate limit are hypothetical and uncommon in nature.

Dehydration, in turn, is the most common volatilization process during metamorphism. High-grade metamorphic rocks have less water than low-grade rocks since rocks tend to expel H_2O during progressive metamorphic reactions. Nonetheless, the maximum F value for oxygen loss is even lower than for decarbonation (Sharp, 2017). Considering the following equations involving muscovite and talc:

$$KAl_3Si_3O_{10}(OH)_2 + SiO_2 \rightarrow KAlSi_3O_8 + Al_2SiO_5 + H_2O$$

muscovite *quartz* *microcline* *kyanite*

$$Mg_3Si_4O_{10}(OH)_2 \rightarrow 3MgSiO_3 + SiO_2 + H_2O$$

talc *enstatite* *quartz*

F values cannot decrease beyond 0.93 and 0.92, respectively (Sharp, 2017). This is equivalent to 7% and 8% of oxygen lost to the fluid phase in these reactions. According to some authors (e.g., Valley, 1986; Sharp, 2017) the effect of $\delta^{18}O$ depletion due to dehydration is commonly less than 1‰.

2.2.2.1.3 Coupled C and O depletion

Coupled volatile reactions are not uncommon as carbon and oxygen frequently evolve simultaneously during the metamorphism of lithologies such as siliceous carbonates and marls (Valley, 1986). The normal calc-silicate decarbonation trend (Figure 7) where F_{oxygen} is equal to 0.6 (meaning that no more than 40% of O from the rock is expelled) will occur if all minerals in the rock are in equilibrium during metamorphic reactions. In these cases, all carbon is released as CO_2 (F_{carbon} = 0 in Figure 7).

If the rock has more than 50% of carbon that is not involved in the reactions, the inert carbon trend will be followed (Figure 7) and consequently, the depletion of $\delta^{13}C$ will be reduced. Similarly, if a rock has a 50% excess of silicate minerals that are not involved in metamorphic reactions, but is isotopically in equilibrium, F_{oxygen} will be 0.8 and F_{carbon} will be zero, following 50% inert oxygen path. However, depletion of $\delta^{18}O$ higher than expected from a normal calc-silicate decarbonation trend can be accomplished by reactions that do not involve silicates, such as the formation of lime from calcite:

$$CaCO_3 \rightarrow CaO + CO_2$$

which follows the silicate absent decarbonation trend in Figure 7. Even higher depletions would be possible if carbonates volatilize in disequilibrium with coexisting silicates (Lattanzi et al., 1980; Lasaga and Rye, 1993).

Valley (1986) summarized 28 studies of marbles affected by contact metamorphism in different localities (Figure 8). All data presents a negative C-O trend, indicating depletion in both stable isotopes. The effect of Rayleigh volatilization alone is insufficient to explain the C and O depletion shown in most studied cases (Figure 8). Fluid infiltration and exchange involving low $\delta^{18}O$ magmatic fluids must be necessary, as seen in data scattering towards igneous values.

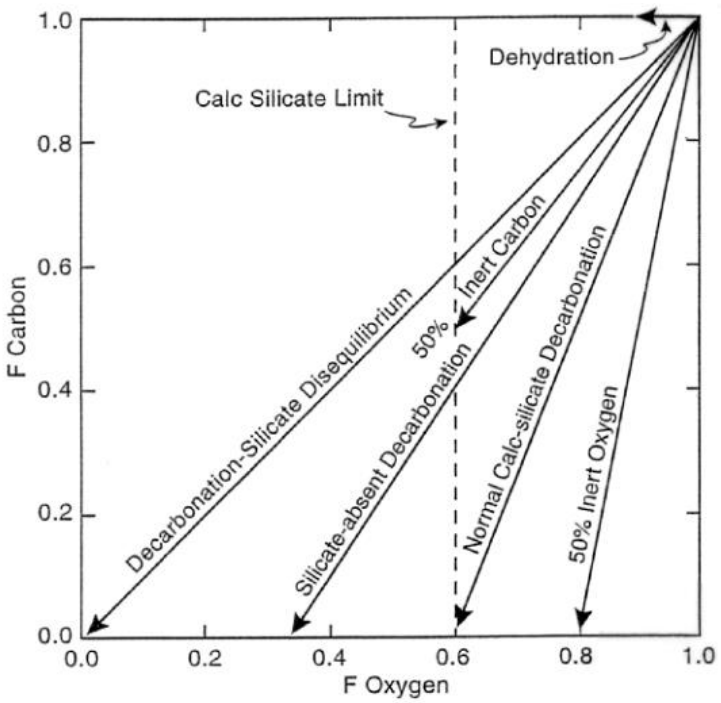

Figure 7 – Values of F for carbon and oxygen for several reaction paths. F is the remaining mole fraction of C or O in the rock. From Valley (1985)

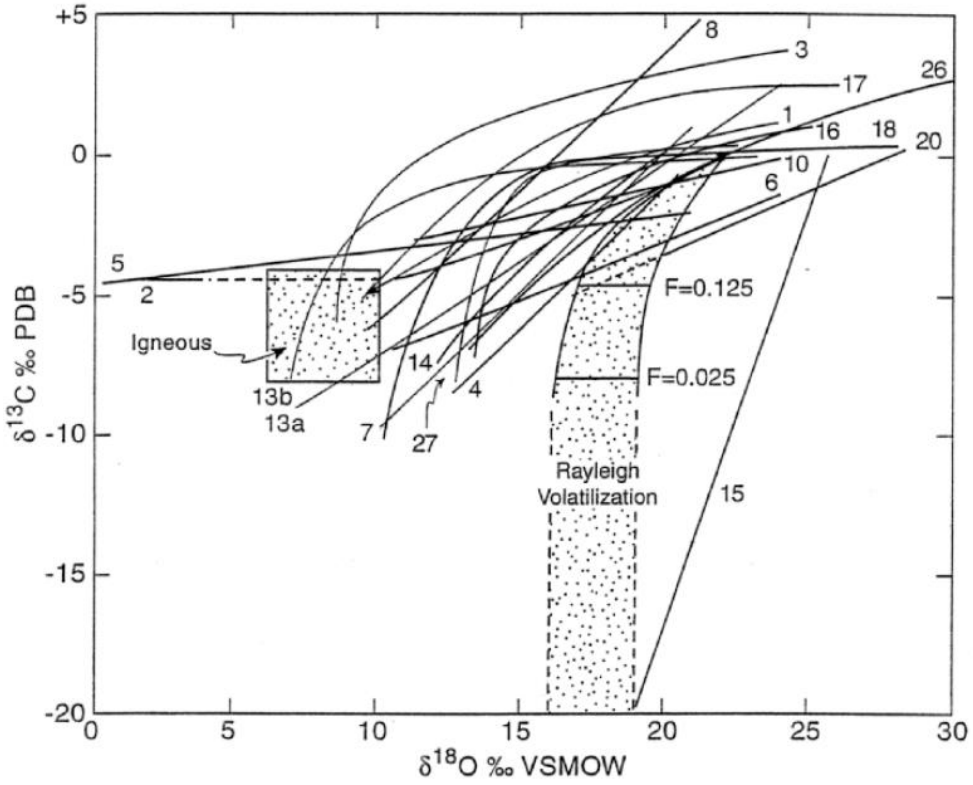

Figure 8 – Coupled carbon and oxygen depletion trends with increasing metamorphic grade (mostly in contact metamorphism settings). Trends going from values of typical marine limestones ($\delta^{18}O$ ranging from 20 to 26‰; $\delta^{13}C$ from -2 to 4‰) towards igneous values. From Baumgartner and Valley (2001).

2.2.3 Fluid-rock interaction and fluid infiltration

As previously mentioned, the effect of volatilization may not be sufficient to explain more significant depletion trends observed in nature. However, these shifts can be derived from exchange with infiltration fluids. The fluid-rock interaction is an exchange of isotopes and elements that occurs at increasing temperatures and involve dissolution-precipitation, chemical exchange reactions, redox reactions, diffusion, and their combinations (Hurai et al., 2015)

Taylor (1974, 1977) modified mass balance equations to calculate the amount of fluid exchanging with surrounding rocks. Assuming an aqueous fluid in a closed system, all fluid completely equilibrates with the rocks undergoing continuous recirculation and cyclic re-equilibrium. In this situation, where fluid and isotopic exchange are only dependent on temperature and water/rock ratio, the mass balance can be calculated using:

$$\frac{W}{R} = \frac{\delta_R^f - \delta_R^i}{\delta_W^i - \delta_R^f + \Delta}$$

where δ_R^f is isotope composition of the rock after exchange; δ_R^i is the initial isotope composition; δ_W^i is the initial isotope composition of the fluid; Δ is the isotope fractionation between rock (or mineral) and fluid that can also be expressed as $\delta_R^f - \delta_W^f$.

In the opposite case, in an open system, where part of the fluid will be lost from the system and each increment of fluid makes only a single pass through the system (Taylor, 1977), the water/rock ratio will be calculated using the following equation:

$$\frac{W}{R} = \ln\left[1 + \left(\frac{W}{R}\right)_{closed}\right]$$

Considering a hydrothermal system altering carbonates, the mixing process only modifies the isotope composition of already existing carbonates without triggering precipitation. The alteration of the isotopic ratio of oxygen in a calcite by an H_2O-rich fluid could be calculated by the following mass balance equation:

$$\frac{W}{R} = \left[\frac{\delta^{18}O_{cal}^f - \delta^{18}O_{cal}^i}{\delta^{18}O_{H_2O}^i - \delta^{18}O_{H_2O}^f + \Delta^{18}O_{cal-H_2O}}\right]$$

Similarly, considering a carbon isotope exchange for different CO_2 concentrations of a hydrothermal fluid-altered calcite, the following expression can be used:

$$\frac{W}{R} \times X_{CO_2} = \left[\frac{\delta^{13}C^{f}_{cal} - \delta^{13}C^{i}_{cal}}{\delta^{13}C^{i}_{CO_2} - \delta^{13}C^{f}_{CO_2} + \Delta^{13}C_{cal-CO_2}} \right]$$

where XCO_2 denotes the molar ratio of CO_2 in the solution and Δ is the equilibrium carbon isotope fractionation between carbonate and CO_2.

As an example of this process, Nabelek et al. (1984) measured the $\delta^{18}O$ and $\delta^{13}C$ values of pure limestones and calcareous argillites intruded by a granitic stock. $\delta^{13}C$ values were depleted by nearly 12‰ whereas $\delta^{18}O$ depletion was almost 11‰. As seen in Figure 9a, all C changes can be explained by batch volatilization or Rayleigh fractionation. In contrast, decarbonation would only lower $\delta^{18}O$ by about 2‰ (Figure 9b), a value significantly below the 11‰ observed. The $\delta^{18}O$ values measured require an open system behavior, explained by infiltration of low $\delta^{18}O$ fluid from crystallizing granite.

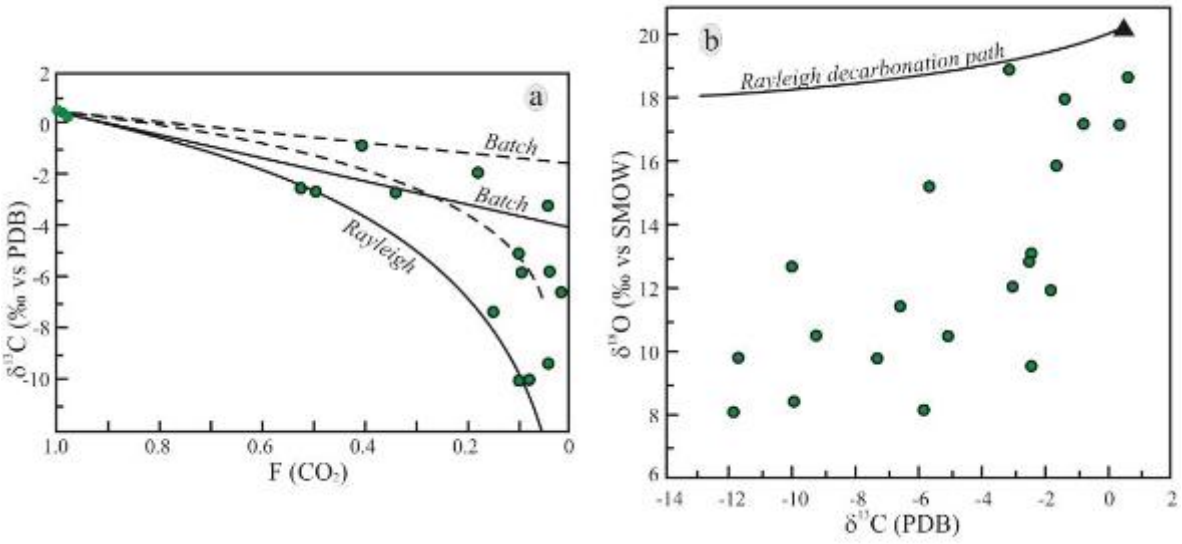

Figure 9 – Isotopic data from limestones and calcareous argillites intruded by Notch Peak Stock, Utah. (a) $\delta^{13}C$ of carbonate as a function of the fraction of CO_2 left in the rock. Dashed and solid lines show theoretical paths of $\delta^{13}C$ depletion for Rayleigh and batch fractionation. (b) $\delta^{18}O$ values near intrusion show lower values than expected for Rayleigh decarbonation. From Nabelek et al. (1984).

3 SÍNTESE E CONSIDERAÇÕES FINAIS

Através da aplicação de diversas metodologias, como análise petrográfica e textural, química mineral, modelagem termodinâmica, isótopos de carbono e oxigênio e geocronologia foi possível propor um modelo para a evolução metamórfica e metassomática do skarn e mármore do Distrito mineral de Bodó. A integração de todas essas técnicas permitiu incrementar de forma significativa o conhecimento até então escasso sobre esse depósito de skarn mineralizado em tungstênio que está entre os mais importantes da Província Mineral Seridó.

A assembleia mineral silicática dos mármores é composta por flogopita, tremolita, diopsídio e granada, podendo estar acompanhada de wollastonita, escapolita e epidoto. Já os skarns apresentam fases de alta temperatura, tais como grossulária, diopsídio e plagioclásio, e fases de baixa temperatura que incluem vesuvianita, epidoto, prehnita, quartzo, calcita e outros minerais. A scheelita, principal mineral explorado, tem sua paragênese inicial associada ao estágios de alta temperatura. Outros minerais portadores de metal importantes são a molibdenita, pirita e calcopirita, que ocorrem comumente em fases mais tardias da evolução do skarn.

Dados isotópicos de carbono e oxigênio obtidos em calcita de skarns e mármores metassomatizados revelam empobrecimento em ambos isótopos (com uma depleção mais acentuada em $\delta^{18}O$) quando comparados com dados de mármores da Formação Jucurutu. Esse empobrecimento, que não pode ser atribuído somente ao mecanismo de descarbonatação dos mármores, é consistente com um modelo de interação fluido-rocha promovido pela interação do substrato com fluidos de origem magmática. Curvas de mistura construídas utilizando o mármore regional (não afetado pelo metassomatismo) e um mebro final magmático indicam um sistema extremamente heterogêneo, percolado por fluidos com variados valore de CO_2 e com diferentes razão fluido:rocha.

As condições de formação das rochas estudadas foram estimadas a partir de pseudosseções T-XCO_2, as quais indicaram uma temperatura máxima de 650-600°C e valores distintos de CO_2, com um estágio retrógrado que se inicia em cerca de 500°C. A presença de minerais de origem metassomática (e.g., granada e escapolita)

está associada a um sistema aberto marcado por variações nos valores de CO_2. A cristalização de escapolita requer um aumento de XCO_2, que pode ocorrer sob condições isotérmicas, enquanto a formação da granada metassomática está relacionada a uma grande diminuição nos valores de XCO_2.

A atividade magmática no distrito é representada por diques de pegmatitos e um granito equigranular. As datações no granito forneceram idade U-Pb em zircão de aproximadamente 537 Ma e idade $^{40}Ar/^{39}Ar$ em biotita de ca. 490 Ma. O pegmatito, por sua vez, teve sua idade de resfriamento estimada em cerca de 500 Ma ($^{40}Ar/^{39}Ar$ em muscovita). A idade da mineralização (Re-Os em molibdenita), porém, é coeva a idades U-Pb em columbita-tantalita obtida em outros pegmatitos da Faixa Seridó (Baumgartner et al., 2006).

REFERÊNCIAS

Archanjo, C.J., Viegas, L.G.F., Hollanda, M.H.B.M., Souza, L.C., and Liu, D., 2013, Timing of the HT/LP transpression in the Neoproterozoic Seridó Belt (Borborema Province, Brazil): Constraints from UPb (SHRIMP) geochronology and implications for the connections between NE Brazil and West Africa: Gondwana Research, v. 23, p. 701–714, doi:10.1016/j.gr.2012.05.005.

Baumgartner, R., Romer, R.L., Moritz, R., Sallet, R., and Chiaradia, M., 2006, Columbite-tantalite-bearing granitic pegmatites from the Seridó Belt, northeastern Brazil: Genetic constraints from U-Pb dating and Pb isotopes: Canadian Mineralogist, v. 44, p. 69–86, doi:10.2113/gscanmin.44.1.69.

Baumgartner, L.P., and Valley, J.W., 2001, Stable Isotope Transport and Contact Metamorphic Fluid Flow: Reviews in Mineralogy and Geochemistry, v. 43, p. 415–467, doi:10.2138/gsrmg.43.1.415.

Beurlen, H., Da Silva, M.R.R., Thomas, R., Soares, D.R., and Olivier, P., 2008, Nb–Ta–(Ti–Sn) oxide mineral chemistry as tracer of rare-element granitic pegmatite fractionation in the Borborema Province, Northeastern Brazil: Mineralium Deposita, v. 43, p. 207–228, doi:10.1007/s00126-007-0152-4.

Beurlen, H., Thomas, R., da Silva, M.R.R., Mu¨ller, A., Rhede, D., and Soares, D.R., 2014, Perspectives for Li- and Ta-Mineralization in the Borborema Pegmatite Province, NE-Brazil: A review: Journal of South American Earth Sciences, v. 56, p. 110–127, doi:10.1016/j.jsames.2014.08.007.

Bottinga, Y., 1969, Calculated fractionation factors for carbon and hydrogen isotope exchange in the system calcite-carbon dioxide-graphite-methane-hydrogen-water vapor: Geochimica et Cosmochimica Acta, v. 33, p. 49–64, doi:10.1016/0016-7037(69)90092-1.

Bowman, J.R., Covert, J.J., Clark, A.H., and Mathieson, G.A., 1985, The CanTung E Zone scheelite skarn orebody, Tungsten, Northwest Territories; oxygen, hydrogen, and carbon isotope studies: Economic Geology, v. 80, p. 1872–1895, doi:10.2113/gsecongeo.80.7.1872.

Bowman, J.R., Willett, S.D., and Cook, S.J., 1994, Oxygen isotopic transport and exchange during fluid flow; one-dimensional models and applications: American Journal of Science, v. 294, p. 1–55, doi:10.2475/ajs.294.1.1.

Brown, P.E., Bowman, J.R., and Kelly, W.C., 1985, Petrologic and stable isotope constraints on the source and evolution of skarn-forming fluids at Pine Creek, California: Economic Geology, v. 80, p. 72–95, doi:10.2113/gsecongeo.80.1.72.

Buriánek, D., Houzar, S., Krmíček, L., and Šmerda, J., 2017, Origin of the pegmatite veins within the skarn body at Vevčice near Znojmo (Gfohl Unit, Moldanubian Zone): Journal of Geosciences, p. 1–23, doi:10.3190/jgeosci.234.

Candela, P.A., 1992, Controls on ore metal ratios in granite-related ore systems: an experimental and computational approach, *in* Geological Society of America

Special Papers, Geological Society of America, v. 272, p. 317–326, doi:10.1130/SPE272-p317.

Cavalcante, R., Cunha, A.L.C. da, Oliveira, R.G. de, Medeiros, V.C., Dantas, A.R., Costa, A.P., Lins, C.A.C., and Larizzatti, J.H., 2016, Metalogenia das Províncias Minerais do Brasil: Área Seridó-Leste, extremo nordeste da Província Borborema (RN-PB): Informe de Recursos Minerais (IRM), v. Série Províncias Minerais do Brasil, p. 105.

Chacko, T., Cole, D.R., and Horita, J., 2001, Equilibrium Oxygen, Hydrogen and Carbon Isotope Fractionation Factors Applicable to Geologic Systems: Reviews in Mineralogy and Geochemistry, v. 43, p. 1–81, doi:10.2138/gsrmg.43.1.1.

Chang, Z., and Meinert, L., 2008, Zonation in skarns - Complexities and controlling factors, *in* PACRIM Congress 2008, Gold Coast, Queensland, Australia, Australasian Institute of Mining and Metallurgy (AusIMM).

Chang, Z., Shu, Q., and Meinert, L.D., 2019, Skarn Deposits of China: Society of Economic Geologists, Special Publication, v. 22, p. 46, doi:10.5382/SP.22.06;

Costa, A.C.D., 1995, Estudos dos processos metassomáticos responsáveis pela mineralização scheelitífera da faixa de Bodó-RN [Relatório de Graduação]: Universidade Federal do Rio Grande do Norte.

Einaudi, M.T., 1982, Description of skarns associated with porphyry copper plutons, *in* Titley, S.R. ed., Advances in geology of the porphyry copper deposits: southwestern North America, Tucson, AZ, University of Arizona Press, p. 139–183, https://azgs.arizona.edu/azgeobib/description-skarns-associated-porphyry-copper-plutons-southwestern-north-america-titley-sr (accessed August 2021).

Einaudi, M.T., and Burt, D.M., 1982, Introduction - terminology, classification, and composition of skarn deposits: Economic Geology, v. 77, p. 745–754, doi:10.2113/gsecongeo.77.4.745.

Elongo, V., Lecumberri-Sanchez, P., Legros, H., Falck, H., Adlakha, E., and Roy-Garand, A., 2020, Paragenetic constraints on the Cantung, Mactung and Lened tungsten skarn deposits, Canada: Implications for grade distribution: Ore Geology Reviews, v. 125, p. 103677, doi:10.1016/j.oregeorev.2020.103677.

Faure, G., Mensing, T.M., and Faure, G., 2005, Isotopes: principles and applications: Hoboken, N.J, Wiley, 897 p.

Frisch, C.J., and Helgeson, H.C., 1984, Metasomatic phase relations in dolomites of the Adamello Alps: American Journal of Science, v. 284, p. 121–185, doi:10.2475/ajs.284.2.121.

Hollanda, M.H.B.M., Archanjo, C.J., Bautista, J.R., and Souza, L.C., 2015, Detrital zircon ages and Nd isotope compositions of the Seridó and Lavras da Mangabeira basins (Borborema Province, NE Brazil): Evidence for exhumation and recycling associated with a major shift in sedimentary provenance:

Precambrian Research, v. 258, p. 186–207, doi:10.1016/j.precamres.2014.12.009.

Hollanda, M.H.B.M., Archanjo, C.J., Souza, L.C., Dunyi, L., and Armstrong, R., 2011, Long-lived Paleoproterozoic granitic magmatism in the Seridó-Jaguaribe domain, Borborema Province–NE Brazil: Journal of South American Earth Sciences, v. 32, p. 287–300, doi:10.1016/j.jsames.2011.02.008.

Hollanda, M.H.B.M., Souza Neto, J.A., Archanjo, C.J., Stein, H., and Maia, A.C.S., 2017, Age of the granitic magmatism and the W-Mo mineralization in skarns of the Seridó belt (NE Brazil) based on zircon U-Pb (SHRIMP) and molybdenite Re-Os dating: Journal of South American Earth Sciences, v. 79, p. 1–11, doi:10.1016/j.jsames.2017.07.011.

Hulsbosch, N., Boiron, M.-C., Dewaele, S., and Muchez, P., 2016, Fluid fractionation of tungsten during granite–pegmatite differentiation and the metal source of peribatholitic W quartz veins: Evidence from the Karagwe-Ankole Belt (Rwanda): Geochimica et Cosmochimica Acta, v. 175, p. 299–318, doi:10.1016/j.gca.2015.11.020.

Hurai, V., Huraiová, M., Slobodník, M., and Thomas, R., 2015, Stable Isotope Geochemistry of Geofluids, *in* Geofluids, Elsevier, p. 293–344, doi:10.1016/B978-0-12-803241-1.00009-5.

Jardim de Sá, E.F., Fuck, R.A., Macedo, M.H.D.F., Peucat, J.J., Kawashita, K., Souza, Z.S.D., and Bertrand, J.M., 1995, Pre-Brasiliano orogenic evolution in the Seridó belt, NE Brazil: conflicting geochronological and structural data: Revista Brasileira de Geociências, v. 25, p. 307–314, doi:10.25249/0375-7536.1995307314.

Jiang, W., Li, H., Evans, N., Wu, J., and Cao, J., 2018, Metal Sources of World-Class Polymetallic W–Sn Skarns in the Nanling Range, South China: Granites versus Sedimentary Rocks? Minerals, v. 8, p. 265, doi:10.3390/min8070265.

Kamvong, T., Zaw, K., and Harris, A., 2006, Geology and geochemistry of the Phu Lon copper-gold skarn deposit at the northern Loei Fold Belt, Northeast Thailand: ASEG Extended Abstracts, v. 2006, p. 1–9, doi:10.1071/ASEG2006ab081.

Korges, M., Weis, P., Lüders, V., and Laurent, O., 2018, Depressurization and boiling of a single magmatic fluid as a mechanism for tin-tungsten deposit formation: Geology, v. 46, p. 75–78, doi:10.1130/G39601.1.

Korzhinskii, D.S., 1968, The theory of metasomatic zoning: Mineralium Deposita, v. 3, doi:10.1007/BF00207435.

Korzhinskii, D.S., 1965, The theory of systems with perfectly mobile components and processes of mineral formation: American Journal of Science, v. 263, p. 193–205, doi:10.2475/ajs.263.3.193.

Kwak, T.A., 1987, W-Sn skarn deposits and related metamorphic skarns and granitoids: Amsterdam, Elsevier, Developments in economic geology 24, 451 p.

Lasaga, A.C., and Rye, D.M., 1993, Fluid flow and chemical reaction kinetics in metamorphic systems: American Journal of Science, v. 293, p. 361–404, doi:10.2475/ajs.293.5.361.

Lattanzi, P., Rye, D.M., and Rice, J.M., 1980, Behavior of 13C and 18O in carbonates during contact metamorphism at Marysville, Montana; implications for isotope systematics in impure dolomitic limestones: American Journal of Science, v. 280, p. 890–906, doi:10.2475/ajs.280.9.890.

Lecumberri-Sanchez, P., Vieira, R., Heinrich, C.A., Pinto, F., and Wälle, M., 2017, Fluid-rock interaction is decisive for the formation of tungsten deposits: Geology, v. 45, p. 579–582, doi:10.1130/G38974.1.

Legrand, J.M., Trindade, I.R., and Melo Jr., G., 1994a, A mineralização scheelitífera de Bodó (RN): Um caso de alteração hidrotermal dentro de um sistema transtensional, *in* Balneário Camboriú.

Legrand, J.M., Trindade, I.R., and Melo Jr., G., 1994b, Silicificação e metassomatismo cálcico na escarnitização da mineralização scheelitífera de Bodó (RN), *in* Balneário Camboriú.

Legros, H. et al., 2019, Multiple fluids involved in granite-related W-Sn deposits from the world-class Jiangxi province (China): Chemical Geology, v. 508, p. 92–115, doi:10.1016/j.chemgeo.2018.11.021.

Legros, H., Lecumberri-Sanchez, P., Elongo, V., Laurent, O., Falck, H., Adlakha, E., and Chelle-Michou, C., 2020, Fluid evolution of the Cantung tungsten skarn, Northwest Territories, Canada: Differentiation and fluid-rock interaction: Ore Geology Reviews, v. 127, p. 103866, doi:10.1016/j.oregeorev.2020.103866.

Lindgren, W., 1925, Metasomatism: Geological Society of America Bulletin, v. 36, p. 247–262, doi:10.1130/GSAB-36-247.

Meinert, L.D., 1997, Application of Skarn Deposit Zonation Models to Mineral Exploration: Exploration & Mining Geology, v. 6.

Meinert, L.D., 1992, Skarns and Skarn Deposits: Geoscience Canada, v. 19.

Meinert, L.D., Dipple, G.M., and Nicolescu, S., 2005, World Skarn Deposits, *in* One Hundredth Anniversary Volume, Society of Economic Geologists, doi:10.5382/AV100.11.

Mrozek, S.A., Chang, Z., Spandler, C., Windle, S., Raraz, C., and Paz, A., 2020, Classifying Skarns and Quantifying Metasomatism at the Antamina Deposit, Peru: Insights from Whole-Rock Geochemistry: Economic Geology, v. 115, p. 177–188, doi:10.5382/econgeo.4698.

Nabelek, P.I., Labotka, T.C., O'Neil, J.R., and Papike, J.J., 1984, Contrasting fluid/rock interaction between the Notch Peak granitic intrusion and argillites and limestones in western Utah: evidence from stable isotopes and phase assemblages: Contributions to Mineralogy and Petrology, v. 86, p. 25–34, doi:10.1007/BF00373708.

Ni, P., Wang, X.-D., Wang, G.-G., Huang, J.-B., Pan, J.-Y., and Wang, T.-G., 2015, An infrared microthermometric study of fluid inclusions in coexisting quartz and wolframite from Late Mesozoic tungsten deposits in the Gannan metallogenic belt, South China: Ore Geology Reviews, v. 65, p. 1062–1077, doi:10.1016/j.oregeorev.2014.08.007.

Pan, J.-Y., Ni, P., and Wang, R.-C., 2019, Comparison of fluid processes in coexisting wolframite and quartz from a giant vein-type tungsten deposit, South China: Insights from detailed petrography and LA-ICP-MS analysis of fluid inclusions: American Mineralogist, v. 104, p. 1092–1116, doi:10.2138/am-2019-6958.

Pat Shanks, W.C., 2014, Stable Isotope Geochemistry of Mineral Deposits, *in* Treatise on Geochemistry, Elsevier, p. 59–85, doi:10.1016/B978-0-08-095975-7.01103-7.

Pirajno, F., 2013, Effects of Metasomatism on Mineral Systems and Their Host Rocks: Alkali Metasomatism, Skarns, Greisens, Tourmalinites, Rodingites, Black-Wall Alteration and Listvenites, *in* Metasomatism and the Chemical Transformation of Rock, Berlin, Heidelberg, Springer Berlin Heidelberg, Lecture Notes in Earth System Sciences, p. 203–251, doi:10.1007/978-3-642-28394-9_7.

Ray, G.E., and Webster, I.C.L., 1991, An overview of skarn deposits, *in* Ore Deposits, Tectonics and Metallogeny in the Canadian Cordillera, Province of British Columbia, Ministry of Energy, Mines, and Petroleum Resources.

Robb, L.J., 2005, Introduction to ore-forming processes: Malden, MA, Blackwell Pub, 373 p.

Rollinson, H.R., and Pease, V., 2021, Using geochemical data: to understand geological processes: Cambridge, UK ; New York, NY, Cambridge University Press.

Romer, R.L., and Kroner, U., 2016, Phanerozoic tin and tungsten mineralization—Tectonic controls on the distribution of enriched protoliths and heat sources for crustal melting: Gondwana Research, v. 31, p. 60–95, doi:10.1016/j.gr.2015.11.002.

Rumble, D., 1982, Stable isotope fractionation during metamorphic devolatilization reactions, *in* Ferry, J.M. ed., Characterization of Metamorphism through Mineral Equilibria, De Gruyter, p. 327–353, doi:10.1515/9781501508172-012.

Santiago, J.S., Souza, V. da S., Dantas, E.L., and Oliveira, C.G. de, 2019, Ediacaran emerald mineralization in Northeastern Brazil: the case of the Fazenda Bonfim Deposit: Brazilian Journal of Geology, v. 49, p. e20190081, doi:10.1590/2317-4889201920190081.

Santos, E., Souza Neto, J., Silva, M., Beurlen, H., Dias Cavalcanti, J., Silva, M., Dias, V., Costa, Á., Santos, L., and Santos, R., 2014, Metalogênese das Porções Norte e Central da Província Borborema, *in* v. 1, p. 343–388.

Sharp, Z., 2017, Principles of Stable Isotope Geochemistry, 2nd Edition:, doi:10.25844/H9Q1-0P82.

Song, S., Mao, J., Zhu, Y., Yao, Z., Chen, G., Rao, J., and Ouyang, Y., 2018, Partial-melting of fertile metasedimentary rocks controlling the ore formation in the Jiangnan porphyry-skarn tungsten belt, south China: A case study at the giant Zhuxi W-Cu skarn deposit: Lithos, v. 304–307, p. 180–199, doi:10.1016/j.lithos.2018.02.002.

Souza, Z.S., Kalsbeek, F., Deng, X.-D., Frei, R., Kokfelt, T.F., Dantas, E.L., Li, J.-W., Pimentel, M.M., and Galindo, A.C., 2016, Generation of continental crust in the northern part of the Borborema Province, northeastern Brazil, from Archaean to Neoproterozoic: Journal of South American Earth Sciences, v. 68, p. 68–96, doi:10.1016/j.jsames.2015.10.006.

Taylor, H.P., 1974, The Application of Oxygen and Hydrogen Isotope Studies to Problems of Hydrothermal Alteration and Ore Deposition: Economic Geology, v. 69, p. 843–883, doi:10.2113/gsecongeo.69.6.843.

Taylor, H.P., 1977, Water/rock interactions and the origin of H2O in granitic batholiths: Thirtieth William Smith lecture: Journal of the Geological Society, v. 133, p. 509–558, doi:10.1144/gsjgs.133.6.0509.

Thompson, J.B., 1959, Local equilibrium in metasomatic processes: Researches in Geochemistry, https://ci.nii.ac.jp/naid/10020475090/ (accessed October 2021).

Valley, J.W., 1986, Stable isotope geochemistry of metamorphic rocks, *in* Valley, J.W., Taylor, H.P., and O'Neil, J.R. eds., Stable Isotopes in High Temperature Geological Processes, Berlin, Boston, De Gruyter, p. 445–490, doi:10.1515/9781501508936-018.

Van Schmus, W.R., Brito Neves, B.B., Williams, I.S., Hackspacher, P.C., Fetter, A.H., Dantas, E.L., and Babinski, M., 2003, The Seridó Group of NE Brazil, a late Neoproterozoic pre- to syn-collisional basin in West Gondwana: insights from SHRIMP U–Pb detrital zircon ages and Sm–Nd crustal residence (TDM) ages: Precambrian Research, v. 127, p. 287–327, doi:10.1016/S0301-9268(03)00197-9.

Zarayskiy, G.P., Zharikov, V.A., Stoyanovskaya, F.M., and Balashov, V.N., 1987, The experimental study of bimetasomatic skarn formation: International Geology Review, v. 29, p. 761–858, doi:10.1080/00206818709466181.

Zhang, W., Jiang, S.-Y., Ouyang, Y., and Zhang, D., 2021, Geochronology and textural and compositional complexity of apatite from the mineralization-related granites in the world-class Zhuxi W-Cu skarn deposit: A record of magma evolution and W enrichment in the magmatic system: Ore Geology Reviews, v. 128, p. 103885, doi:10.1016/j.oregeorev.2020.103885.

Zharikov, V.A., 1970a, Skarns (Part I): International Geology Review, v. 12, p. 541–559, doi:10.1080/00206817009475262.

Zharikov, V.A., 1970b, Skarns (Part II): International Geology Review, v. 12, p. 619–647, doi:10.1080/00206817009475270.

Zharikov, V.A., Pertsev, N.N., Rusinov, V.L., Callegari, E., and Fettes, D.J., 2007, Metasomatism and metasomatic rocks, *in* Recommendations by the IUGS Subcommission on the systematics of metamorphic rocks, British Geological Survey, https://www2.bgs.ac.uk/downloads/start.cfm?id=3193.

Zharikov, V.A., and Rusinov, V.L., 2015, Metasomatism and metasomatic rocks:, http://apps.earthsciences.iupui.edu:3838/RockR/Info/Metasomatism.pdf.

Zheng, Y.-F., 1999, Oxygen isotope fractionation in carbonate and sulfate minerals.: Geochemical Journal, v. 33, p. 109–126, doi:10.2343/geochemj.33.109.